

## Experimental observation of two massless Dirac-fermion gases in graphene-topological insulator heterostructure

This content has been downloaded from IOPscience. Please scroll down to see the full text.

2016 2D Mater. 3 021009

(<http://iopscience.iop.org/2053-1583/3/2/021009>)

View [the table of contents for this issue](#), or go to the [journal homepage](#) for more

Download details:

IP Address: 140.109.101.40

This content was downloaded on 05/04/2017 at 04:35

Please note that [terms and conditions apply](#).

You may also be interested in:

[Topological insulators, topological superconductors and Weyl fermion semimetals: discoveries, perspectives and outlooks](#)

M Zahid Hasan, Su-Yang Xu and Guang Bian

[Chemical and electronic structure imaging of graphene on Cu: a NanoARPES study](#)

Chaoyu Chen, José Avila and Maria C Asensio

[Topological phases in two-dimensional materials: a review](#)

Yafei Ren, Zhenhua Qiao and Qian Niu

[The helical surface states of the S-covered topological insulator Sb<sub>2</sub>Te<sub>3</sub>\(0001\)](#)

Xu Zhao, Xian-Qi Dai, Bao Zhao et al.

[Scanning tunneling microscopy studies of topological insulators](#)

Kun Zhao, Yan-Feng Lv, Shuai-Hua Ji et al.

[Electronic properties of graphene: a perspective from scanning tunneling microscopy and magnetotransport](#)

Eva Y Andrei, Guohong Li and Xu Du

[Heavy Dirac fermions in a graphene/topological insulator hetero-junction](#)

Wendong Cao, Rui-Xing Zhang, Peizhe Tang et al.

[Electronic structure of transferred graphene/h-BN van der Waals heterostructures with nonzero stacking angles by nano-ARPES](#)

Eryin Wang, Guorui Chen, Guoliang Wan et al.

## 2D Materials



### LETTER

# Experimental observation of two massless Dirac-fermion gases in graphene-topological insulator heterostructure

RECEIVED  
5 February 2016

REVISED  
4 April 2016

ACCEPTED FOR PUBLICATION  
26 April 2016

PUBLISHED  
11 May 2016

Guang Bian<sup>1,12</sup>, Ting-Fung Chung<sup>2,3,12</sup>, Chaoyu Chen<sup>4,12</sup>, Chang Liu<sup>1,5,12</sup>, Tay-Rong Chang<sup>1,6</sup>, Tailung Wu<sup>2,3</sup>, Ilya Belopolski<sup>1</sup>, Hao Zheng<sup>1</sup>, Su-Yang Xu<sup>1</sup>, Daniel S Sanchez<sup>1</sup>, Nasser Alidoust<sup>1</sup>, Jonathan Pierce<sup>7</sup>, Bryson Quilliams<sup>7</sup>, Philip P Barletta<sup>7</sup>, Stephane Lorcy<sup>4</sup>, José Avila<sup>4</sup>, Guoqing Chang<sup>8,9</sup>, Hsin Lin<sup>8,9</sup>, Horng-Tay Jeng<sup>6,10</sup>, Maria-Carmen Asensio<sup>4</sup>, Yong P Chen<sup>2,3,11</sup> and M Zahid Hasan<sup>1</sup>

<sup>1</sup> Laboratory for Topological Quantum Matter and Spectroscopy (B7), Department of Physics, Princeton University, Princeton, NJ 08544, USA; Department of Physics and Astronomy, University of Missouri, Columbia, Missouri 65211, USA

<sup>2</sup> Department of Physics and Astronomy, Purdue University, West Lafayette, IN 47907, USA

<sup>3</sup> Birck Nanotechnology Center, Purdue University, West Lafayette, IN 47907, USA

<sup>4</sup> Synchrotron SOLEIL, L'Orme des Merisiers, Saint-Aubin—BP48, F-91192 GIF-sur-YVETTE CEDEX, France

<sup>5</sup> Department of Physics, South University of Science and Technology of China, Shenzhen, Guangdong 518055, People's Republic of China

<sup>6</sup> Department of Physics, National Tsing Hua University, Hsinchu 30013, Taiwan

<sup>7</sup> Center for Solid State Energetics, RTI International, Research Triangle Park, NC 27709, USA

<sup>8</sup> Centre for Advanced 2D Materials and Graphene Research Centre National University of Singapore, 6 Science Drive 2, 117546, Singapore

<sup>9</sup> Department of Physics, National University of Singapore, 2 Science Drive 3, 117542, Singapore

<sup>10</sup> Institute of Physics, Academia Sinica, Taipei 11529, Taiwan

<sup>11</sup> School of Electrical and Computer Engineering, Purdue University, West Lafayette, IN 47907, USA

<sup>12</sup> These authors contributed equally to this work.

E-mail: [maria-carmen.asensio@synchrotron-soleil.fr](mailto:maria-carmen.asensio@synchrotron-soleil.fr), [yongchen@purdue.edu](mailto:yongchen@purdue.edu) and [mzhasan@princeton.edu](mailto:mzhasan@princeton.edu)

Keywords: graphene, topological insulator, proximity effect, heterostructure, ARPES

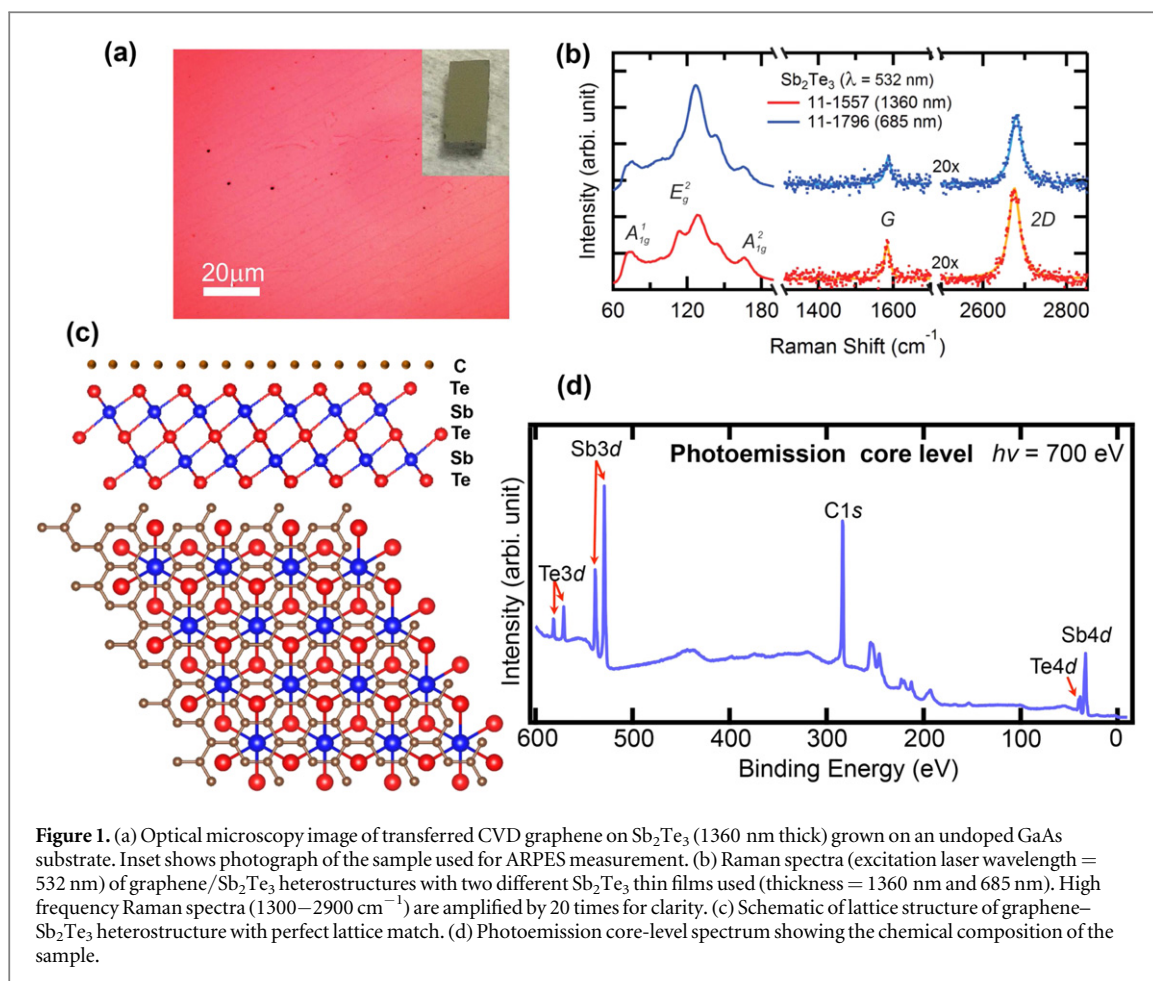
### Abstract

Graphene and topological insulators (TI) possess two-dimensional (2D) Dirac fermions with distinct physical properties. Integrating these two Dirac materials in a single device creates interesting opportunities for exploring new physics of interacting massless Dirac fermions. Here we report on a practical route to experimental fabrication of graphene–Sb<sub>2</sub>Te<sub>3</sub> heterostructure. The graphene–TI heterostructures are prepared by using a dry transfer of chemical-vapor-deposition grown graphene film. ARPES measurements confirm the coexistence of topological surface states of Sb<sub>2</sub>Te<sub>3</sub> and Dirac  $\pi$  bands of graphene, and identify the twist angle in the graphene–TI heterostructure. The results suggest a potential tunable electronic platform in which two different Dirac low-energy states dominate the transport behavior.

### Introduction

Dirac materials such as graphene and topological insulators (TI) have been in the spotlight attracting global research interest in the past decade, because they not only provide unprecedented opportunities to explore fundamental physics in condensed matters but also open a new route for device innovations thanks to the unique electronic properties of those materials [1–10]. In both graphene and TIs, the low-energy excitations can be described as a two-dimensional (2D) electron gas with linear dispersion akin to massless Dirac fermions. There is a key difference between the two systems: in graphene the intrinsic

spin-orbit coupling (SOC) is negligibly small and the chirality of the Dirac state is associated with the sublattice degrees freedom, the so-called pseudospin; on the other hand, in TIs the topological bulk band ordering is caused by the strong SOC and gives rise to the helical spin-momentum locked feature of the Dirac surface states. There have emerged many interesting proposals of combining the two Dirac materials in heterostructures, taking advantage of the dramatic difference in spin texture of their Dirac states [11–15]. It has been predicted that the SOC of graphene can be greatly enhanced by proximity to the strongly spin-orbit coupled TI surface. As a consequence, the epitaxial graphene can develop a spin-orbit gap as



large as 20 meV, making it a Kane–Mele quantum spin–Hall insulator [13, 16]. Thus the major interest in this type of heterojunctions is the potential for engineering electronic structure of graphene by proximity effect. Despite several experimental efforts to grow TI films on graphene substrate [17–19] the experimental fabrication of a graphene layer on top of TI surface remains a tremendous technical challenge, not to mention the characterization of the electronic band structure of such graphene–TI junctions. The difficulty lies in the fact graphene can not be directly grown *in situ* on the surface of TIs such as  $\text{Bi}_2\text{Se}_3$  and  $\text{Sb}_2\text{Te}_3$ . In this work we report on an experimental route to preparing graphene– $\text{Sb}_2\text{Te}_3$  heterostructures in laboratory. We also perform angle-resolved photoemission (ARPES) measurements on the graphene–TI heterostructure and demonstrate the coexistence of two Dirac modes of different types. The results suggest a potential tunable electronic platform for studying the interaction between two different Dirac low-energy states.

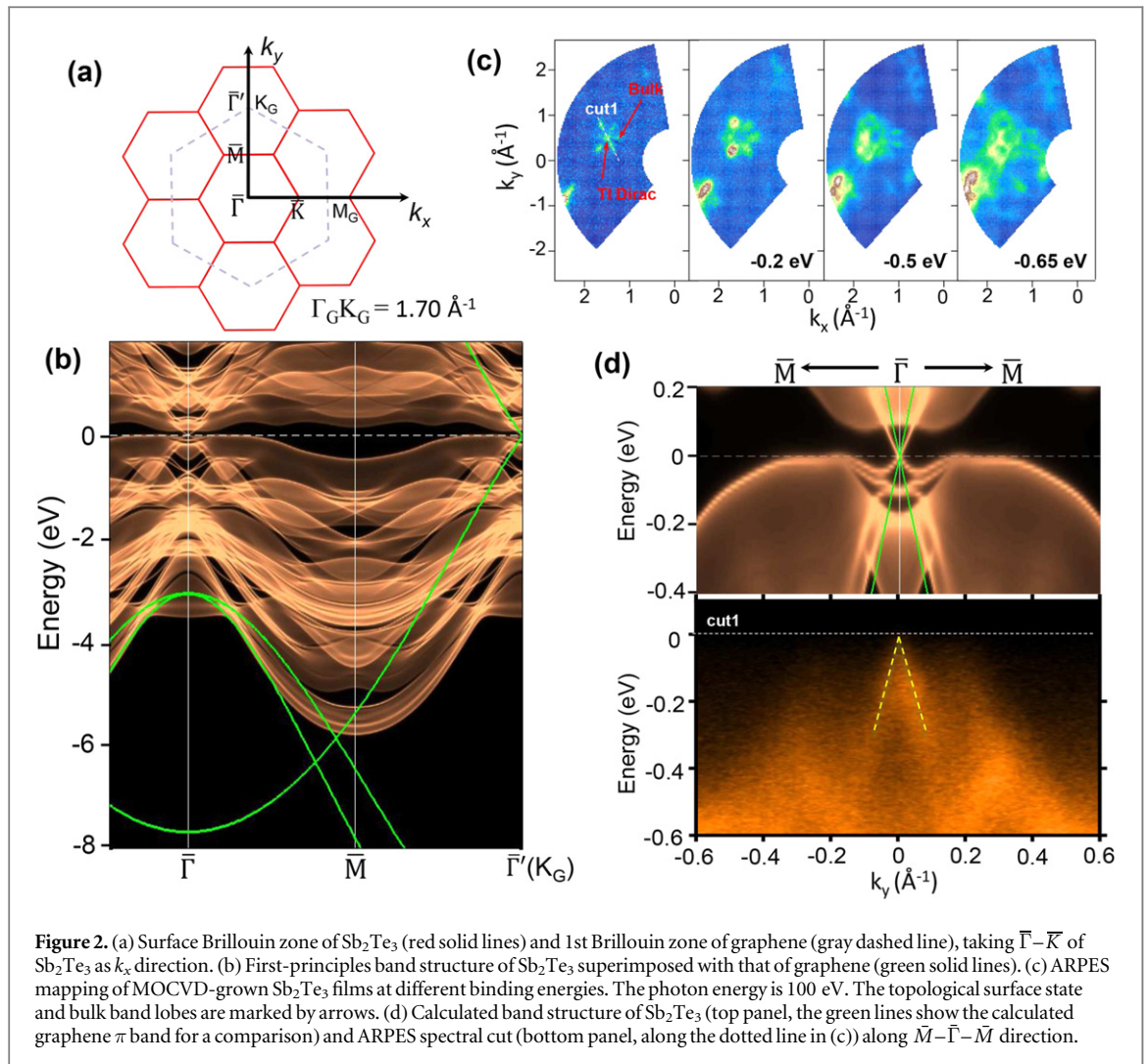
## Results and discussion

The micro-ARPES experiments were carried out at the ANTARES beamline at the SOLEIL synchrotron

with a beam spot size of 50–100  $\mu\text{m}$  [20–23]. The photoelectron spectra were obtained using a hemispherical analyzer Scienta R4000 with 5 meV and 0.005  $\text{\AA}^{-1}$ , energy and momentum resolutions, respectively. The Scienta detector is aligned along the  $\Gamma$ – $K$  direction of graphene. All photoemission measurements at ANTARES were done at a temperature of 100 K. The samples were degassed *in situ* at 200  $^\circ\text{C}$  for 8 h before ARPES measurements. The degassing was proved to be critical for acquiring good ARPES spectra.

The first-principles calculations were based on the generalized gradient approximation [24] using the full-potential projected augmented wave method [25] as implemented in the VASP package [26]. The electronic structure of bulk  $\text{Sb}_2\text{Te}_3$  were calculated using a  $15 \times 15 \times 6$  Monkhorst-Pack  $k$ -mesh over the Brillouin zone (BZ) with the spin–orbit coupling included self-consistently. The surface states were calculated from the surface Green’s function of the semi-infinite system [27]. A  $30 \times 30 \times 1$  Monkhorst-Pack  $k$ -mesh was used in the calculation for graphene.

We choose  $\text{Sb}_2\text{Te}_3$  as the TI substrate because there is a nearly perfect lattice match between the (111) surface of  $\text{Sb}_2\text{Te}_3$  ( $a = 4.26 \text{ \AA}$ ) and a  $\sqrt{3} \times \sqrt{3}$  super cell of graphene ( $a = 2.46 \text{ \AA}$ ). Therefore the heterostructure in the perfect alignment can be described by



a commensurate  $\sqrt{3} \times \sqrt{3}$  stacking pattern. Graphene/ $\text{Sb}_2\text{Te}_3$  heterostructures were prepared using a dry transfer of chemical vapor deposition (CVD) grown graphene film [28]. Graphene film was grown on Cu foils at ambient pressure which has been reported elsewhere [29–31]. Briefly, the growth was at 1065 °C with 20 sccm methane (500 ppm in Ar) and 200 sccm forming gas (5%  $\text{H}_2$  in Ar) for 60–75 min. Prior to the growth, clean Cu foil was annealed for 120 min in the forming gas environment. The  $\text{Sb}_2\text{Te}_3$  thin film was grown (at RTI International) on an undoped GaAs(100) substrate by metalorganic chemical vapor deposition (MOCVD) process. To transfer as-grown graphene film, a PMMA layer was spin-coated onto one side of the Cu foil, and the graphene on the opposite side of the Cu foil was removed by oxygen plasma. Next, a piece of wafer dicing tape (Blue Med Tack Squares from Semiconductor Equipment Corp.) with a small window cut in its center was adhered to the graphene covered with PMMA. The exposed Cu was then dissolved in ammonium persulfate solution (~2.5 g in 50 ml DI water), obtaining a suspended PMMA/graphene membrane. After Cu etching, the sample was further cleaned by DI water and SC2 baths

( $\text{HCl}:\text{H}_2\text{O}_2:\text{H}_2\text{O} = 1:1:50$  ml). The sample is subsequently rinsed by isopropanol and blown dry with  $\text{N}_2$  gas. The typical domain size of graphene is about 20  $\mu\text{m}$  [31]. Finally, the suspended sample was transferred onto  $\text{Sb}_2\text{Te}_3$  substrate, and followed by dissolving the PMMA layer in acetone. Figure 1(a) shows an optical micrograph of the surface of graphene/ $\text{Sb}_2\text{Te}_3$  (thickness of  $\text{Sb}_2\text{Te}_3 = 1360$  nm).

A Horiba Jobin Yvon XploRA confocal Raman system with a solid-state laser operating at a wavelength of 532 nm and a spectral resolution of  $1.1\text{ cm}^{-1}$  was used for the Raman spectroscopy measurement. Power of the laser was maintained below 1 mW to minimize local heating effect. The laser spot size was 0.6  $\mu\text{m}$  in diameter with a 100 $\times$  objective (NA = 0.90) and all measurements were performed in an air ambient environment and at room temperature. As shown in figure 1(b), there are two high-frequency Raman modes at 1584 and 2676  $\text{cm}^{-1}$  in the Raman spectra, corresponding to the G and 2D modes of graphene [32]. We also observe a series of characteristic Raman modes at 73  $\text{cm}^{-1}$  ( $A_{1g}^1$ ), 113  $\text{cm}^{-1}$  ( $E_g^2$ ) and 166  $\text{cm}^{-1}$  ( $A_{1g}^2$ ) for  $\text{Sb}_2\text{Te}_3$  [33]. Two extra peaks could be associated with surface oxidation of the  $\text{Sb}_2\text{Te}_3$  thin film. The measured

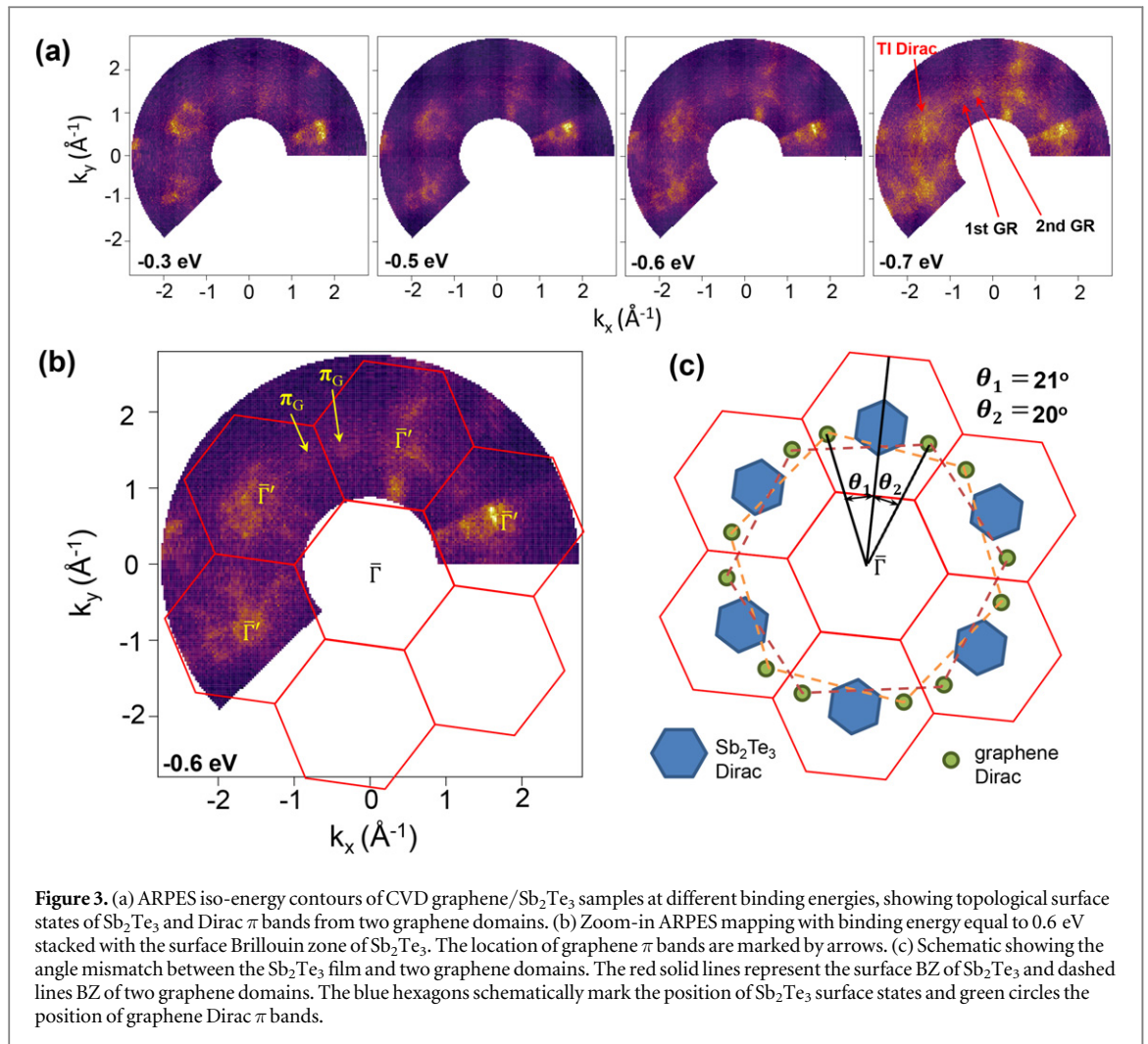
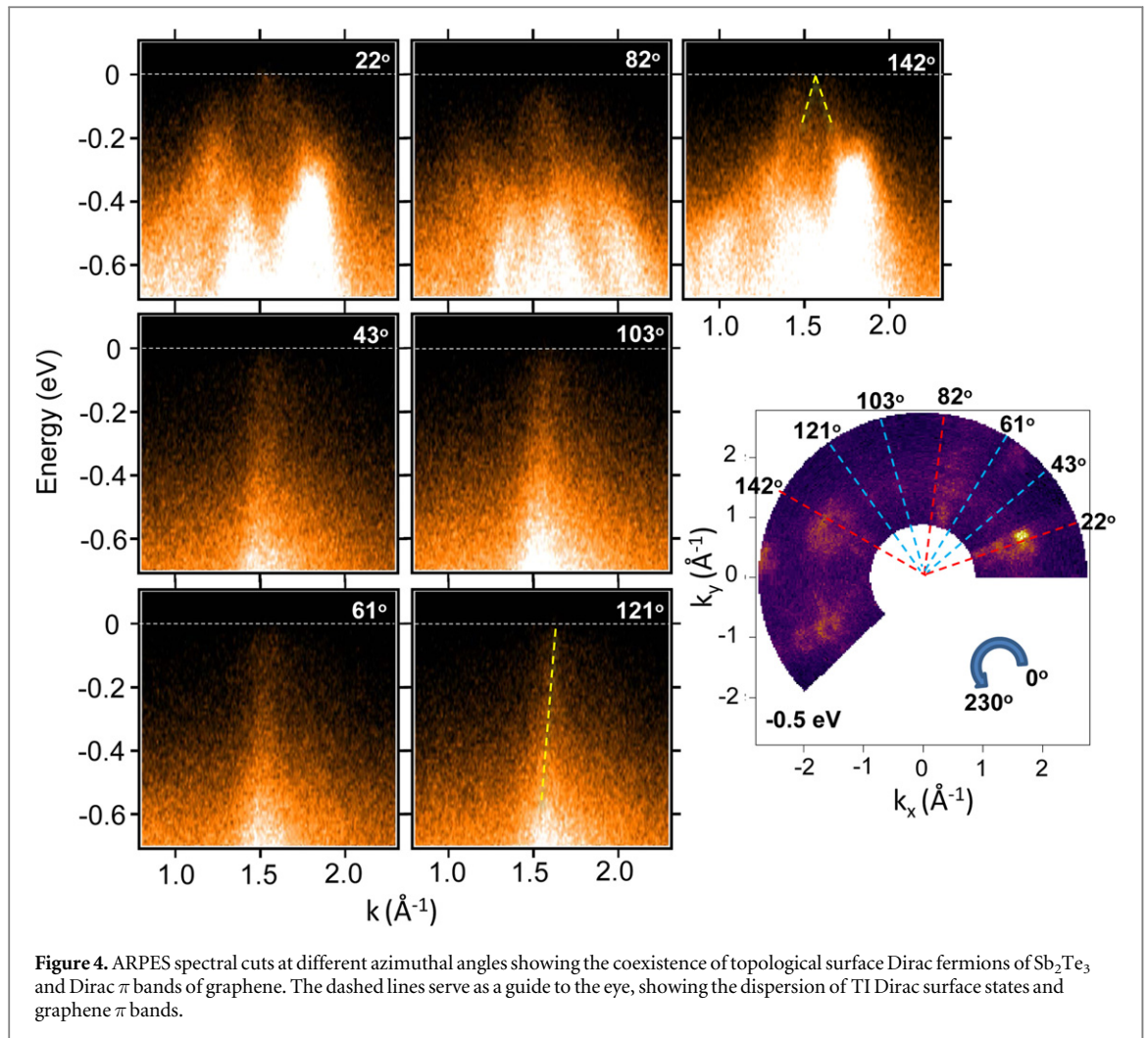


**Figure 3.** (a) ARPES iso-energy contours of CVD graphene/Sb<sub>2</sub>Te<sub>3</sub> samples at different binding energies, showing topological surface states of Sb<sub>2</sub>Te<sub>3</sub> and Dirac  $\pi$  bands from two graphene domains. (b) Zoom-in ARPES mapping with binding energy equal to 0.6 eV stacked with the surface Brillouin zone of Sb<sub>2</sub>Te<sub>3</sub>. The location of graphene  $\pi$  bands are marked by arrows. (c) Schematic showing the angle mismatch between the Sb<sub>2</sub>Te<sub>3</sub> film and two graphene domains. The red solid lines represent the surface BZ of Sb<sub>2</sub>Te<sub>3</sub> and dashed lines BZ of two graphene domains. The blue hexagons schematically mark the position of Sb<sub>2</sub>Te<sub>3</sub> surface states and green circles the position of graphene Dirac  $\pi$  bands.

Raman characteristics confirm the success in fabricating graphene/Sb<sub>2</sub>Te<sub>3</sub> heterostructures.

The lattice structure of graphene/Sb<sub>2</sub>Te<sub>3</sub> with a perfect alignment is plotted in figure 1(c). In this case the surface unit cell of the heterostructure is same as that of Sb<sub>2</sub>Te<sub>3</sub>. However, in reality, there is no epitaxial relationship between CVD graphene and Sb<sub>2</sub>Te<sub>3</sub> and being van der Waals coupled they can be oriented in any angles. Figure 1(d) shows the photoemission spectrum taken with 700 eV photons. The characteristic core levels of C, Sb, and Te atoms are observed, indicating the correct chemical composition of the samples. We note that in the spectrum there exist several extra peaks which can be attributed to the contamination introduced during the *ex situ* assembly of the heterostructure. The surface contamination is mainly from three sources: (1) surface oxidation of the Sb<sub>2</sub>Te<sub>3</sub> surface; (2) inorganic molecules introduced by the Cu etching and bath washing: ammonium persulfate ((NH<sub>4</sub>)<sub>2</sub>S<sub>2</sub>O<sub>8</sub>), hydrochloric acid (HCl) and hydrogen peroxide (H<sub>2</sub>O<sub>2</sub>), which probably explains the photoemission peaks around 200 eV (Cl-2p), 230 eV (S-2s) and 270 eV (Cl-2s); (3) remnant polymer molecules after dissolving the PMMA layer in acetone.

The Brillouin zone corresponding the stacking geometry in figure 1(c) is shown in figure 2(a). The  $K$  point of graphene (where the Dirac point of graphene is located) coincide with the  $\bar{\Gamma}$  point of Sb<sub>2</sub>Te<sub>3</sub> in the second zone. Under this ideal situation the Dirac cones of graphene and Sb<sub>2</sub>Te<sub>3</sub> overlap in momentum space, and strong interaction between the Dirac states is expected. In the nonideal case which there exists an angle mismatch, the Dirac cones of two materials separate in  $k$  space and the interaction between them is weaker. Therefore this is a tunable system (depending on the twist angle) for studying the correlation between two Dirac low-energy modes and the resulting novel transport behaviors. First-principles band structure of Sb<sub>2</sub>Te<sub>3</sub> superimposed with that of graphene (green solid lines) is shown in figure 2(b). We can find that the Dirac cone of graphene indeed overlap with the topological surface states of Sb<sub>2</sub>Te<sub>3</sub>. Figure 2(c) presents ARPES mapping of a Sb<sub>2</sub>Te<sub>3</sub> film employed as the substrate in our experiment (without *in situ* cleavage). The mapping at the Fermi level clearly resolve the Dirac point of the topological surface states and six lobes of bulk valence band as marked by arrows, indicating the good surface quality



of the MOCVD-grown  $\text{Sb}_2\text{Te}_3$  film despite a brief exposure to the air (which is inevitable during the transfer of graphene). A comparison of the ARPES spectrum of  $\text{Sb}_2\text{Te}_3$  with the calculated band structure is given in figure 2(d). It is shown in the APRES spectrum that the Fermi level cuts the topological surface bands at the Dirac point and grazes the top of the bulk valence band, consistent with the first-principles result.

ARPES results taken from our graphene/ $\text{Sb}_2\text{Te}_3$  sample are shown in figure 3(a). Comparing with the result from the bare  $\text{Sb}_2\text{Te}_3$  surface, there are two additional bright spots in the ARPES spectra of the heterostructure, as indicated by the arrows. They are from the  $\pi$  band of graphene. The two spots indicate there are two major domains with different angles of twist in the CVD graphene layer. The twisting geometry of the sample is illustrated in figures 3(b) and (c). According to the ARPES spectra, the distance between the Dirac band of graphene and the zone center is equal to the momentum of  $\text{Sb}_2\text{Te}_3$  surface states in the second zone, which confirms the lattice match of the two Dirac materials. The twist angles of two graphene domains with respect to  $\text{Sb}_2\text{Te}_3$  are  $21^\circ$

and  $20^\circ$ , respectively. To further show the energy dispersion of Dirac fermions in this heterostructure, ARPES spectral cuts are plotted with different azimuthal angles (as marked by the dashed lines in the panel on the right hand side) in figure 4. At angles of  $22^\circ$ ,  $82^\circ$ , and  $142^\circ$ , the Dirac surface states of  $\text{Sb}_2\text{Te}_3$  were observed. We note that the quality of the spectrum is worse than that reported in figure 2, which can be attributed to the coverage of graphene as well as the contamination introduced during the transfer of graphene. At  $43^\circ$  and  $103^\circ$  we saw the linear Dirac  $\pi$  bands from one graphene domain. The  $\pi$  bands of the other graphene domain was observed at  $62^\circ$  and  $122^\circ$ . The Fermi velocity of the CVD graphene is found to be  $(1.01 \pm 0.12) \times 10^8 \text{ cm s}^{-1}$ . In the spectral cuts only one branch of the graphene  $\pi$  band shows up, see figure 4. It is due to a well-known selection rule of photoexcitation matrix elements [9, 34, 35]. The ARPES cuts confirm the twisting geometry schematic shown in figure 3(c) and the coexistence of two different Dirac modes in our graphene/ $\text{Sb}_2\text{Te}_3$  samples, which is the key conclusion of the this work.

## Conclusions

In this work, we explored a practical approach to fabricating graphene/TI heterostructure, a promising platform for studying interacting Dirac fermions. Our ARPES experiment demonstrated the coexistence of the Dirac low-energy states of graphene and  $\text{Sb}_2\text{Te}_3$  in our lab-prepare sample. A twist angle between the CVD graphene layer and the TI substrate was identified by our photoemission measurement. This twist angle provides a tunable degree of freedom for manipulating the electronic properties of the heterojunction system. Our work presented a first step towards an ideal system of two interacting Dirac fermions with a tunable interaction strength. Further improvements on the sample preparation are desired: first, reduce the contamination introduced during the transfer of graphene; second, increase the domain size of graphene; and third, a precise way to control the twist angle. Those efforts will refine the graphene/TI system in such a way that could eventually enable the observation of the proximity effect on the graphene  $\pi$  band and potentially the quantum spin-Hall effect proposed in the original Kane–Mele model of graphene.

## Acknowledgments

This work is supported by the US National Science Foundation (NSF) under Grant No. NSF-DMR-1006492 (MZH). Work at Princeton, Purdue and RTI are also supported by DARPA MESO program (grant N66001-11-1-4107). TFC and YPC also acknowledge support of NSF DMR (grant 0847638) on graphene research. TFC acknowledges financial support from Purdue University through Bilsland Dissertation Fellowship. TRC acknowledges visiting scientist support from Princeton University. The Synchrotron SOLEIL is supported by the Centre National de la Recherche Scientifique (CNRS) and the Commissariat à l'Énergie Atomique at aux Énergies Alternatives (CEA), France. TRC and HTJ are supported by the Ministry of Science and Technology, National Tsing Hua University, and Academia Sinica, Taiwan. We also thank NCHC, CINC-NTU and NCTS, Taiwan for technical support.

## References

- [1] Hasan M Z, Xu S Y and Bian G 2015 *Phys. Scr.* **T164** 014001
- [2] Hasan M Z and Kane C L 2010 *Rev. Mod. Phys.* **82** 3045

- [3] Qi X L and Zhang S C 2011 *Rev. Mod. Phys.* **83** 1057
- [4] Castro Neto A H, Guinea F, Peres N M R, Novoselov K S and Geim A K 2009 *Rev. Mod. Phys.* **81** 109
- [5] Katsnelson M I, Novoselov K S and Geim A K 2006 *Nat. Phys.* **2** 620
- [6] Novoselov K S, Geim A K, Morozov S V, Jiang D, Katsnelson M I, Grigorieva I V, Dubonos S V and Firsov A A 2005 *Nature* **438** 197
- [7] Zhang Y, Tan Y W, Stormer H L and Kim P 2005 *Nature* **438** 201
- [8] Zhou S Y, Gweon G H, Graf J, Fedorov A V, Spataru C D, Diehl R D, Kopelevich Y, Lee D H, Louie S G and Lanzara A 2006 *Nat. Phys.* **2** 595
- [9] Bostwick A, Ohta T, Seyller T, Horn K and Rotenberg E 2006 *Nat. Phys.* **3** 36
- [10] Liu Y, Zhang L, Brinkley M K, Bian G, Miller T and Chiang T C 2010 *Phys. Rev. Lett.* **105** 136804
- [11] Coy-Diaz H, Avila J, Chen C, Addou R, Asensio M C and Batzill M 2015 *ACS Nano* **15** 1135
- [12] Zhang J, Triola C and Rossi E 2014 *Phys. Rev. Lett.* **112** 096802
- [13] Jin K H and Jhi S H 2013 *Phys. Rev. B* **87** 075442
- [14] Qiao Z, Ren W, Chen H, Bellaiche L, Zhang Z, MacDonald A H and Niu Q 2014 *Phys. Rev. Lett.* **112** 116404
- [15] Zhang C *et al* 2014 *Cryst. Eng. Commun.* **16** 8941
- [16] Kane C L and Mele E J 2005 *Phys. Rev. Lett.* **95** 226801
- [17] Zhang Y *et al* 2010 *Nat. Phys.* **6** 584
- [18] Jiang Y *et al* 2012 *Phys. Rev. Lett.* **108** 066809
- [19] Dang W, Peng H, Li H, Wang P and Liu Z 2010 *Nano Lett.* **10** 2870
- [20] Avila J, Rizado-Colambo I, Lorcy S, Lagarde B, Giorgetta J L, Polack F and Asensio M C 2013 *J. Phys. Conf. Ser.* **425** 192023
- [21] Avila J, Rizado-Colambo I, Lorcy S, Fleurier R, Pichonat E, Vignaud D, Wallart X and Asensio M C 2013 *Sci. Rep.* **3** 2439
- [22] Avila J and Asensio M C 2014 *Synchrotron Radiat. News* **27** 24
- [23] Chen C, Avila A, Frantzeskakis E, Levy A and Asensio M C 2015 *Nat. Commun.* **6** 8585
- [24] Perdew J P, Burke K and Ernzerhof M 1996 *Phys. Rev. Lett.* **77** 3865
- [25] Blöchl P E 1994 *Phys. Rev. B* **50** 17953
- [26] Kress G and Hafner J 1993 *Phys. Rev. B* **48** 13115
- [27] Zhang H J, Liu C X, Qi X L, Dai X, Fang Z and Zhang S C 2009 *Nat. Phys.* **5** 438
- [28] Petrone N, Dean C R, Meric I, van der Zande A M, Huang P Y, Wang L, Muller D, Shepard K L and Hone J 2012 *Nano Lett.* **12** 2751
- [29] Cao H *et al* 2010 *App. Phys. Lett.* **96** 122106
- [30] Wu W, Liu Z, Jauregui L A, Yu Q, Bao J, Pillai R, Cao H, Chen Y P and Pei S S 2010 *Sensors Actuators B* **150** 296
- [31] Chung T F, Shen T, Cao H, Jauregui L A, Wu W, Yu Q, Newell D and Chen Y P 2013 *Int. J. Mod. Phys. B* **27** 1341002
- [32] Malard L M, Pimenta M A, Dresselhaus G and Dresselhaus M S 2009 *Phys. Rep.* **473** 51
- [33] Richter W, Krost A, Nowak U and Anastassakis E 1982 *Z. Phys. B: Condens. Matter* **49** 191
- [34] Liu Y, Bian G, Miller T and Chiang T C 2011 *Phys. Rev. Lett.* **107** 166803
- [35] Bian G, Zhang L, Liu Y, Miller T and Chiang T C 2012 *Phys. Rev. Lett.* **108** 186403